Relaxation dynamics of nucleosomal DNA

ARTICLE *in* PHYSICAL CHEMISTRY CHEMICAL PHYSICS · DECEMBER 2009

Impact Factor: 4.49 · DOI: 10.1039/b910937b · Source: PubMed

3 AUTHORS:

Sergei Y Ponomarev
Worcester Polytechnic Institute
20 PUBLICATIONS **304** CITATIONS
SEE PROFILE

Vakhtang Putkaradze
University of Alberta
66 PUBLICATIONS **509** CITATIONS
SEE PROFILE

Thomas C. Bishop
Louisiana Tech University
43 PUBLICATIONS **684** CITATIONS
SEE PROFILE

This paper is published as part of a PCCP Themed Issue on:

Nucleic Acid Simulations

Guest Editors: Modesto Orozco and Charles Laughton

Editorial

Nucleic Acid Simulations
Modesto Orozco and Charles Laughton, *Phys. Chem. Chem. Phys.*, 2009
DOI: 10.1039/b921472k

Perspectives

Viral assembly: a molecular modeling perspective
Stephen C. Harvey, Anton S. Petrov, Batsal Devkota and Mustafa Burak Boz, *Phys. Chem. Chem. Phys.*, 2009
DOI: 10.1039/b912884k

Simulation of DNA catenanes
Alexander Vologodskii and Valentin V. Rybenkov, *Phys. Chem. Chem. Phys.*, 2009
DOI: 10.1039/b910812b

Papers

Stabilization of radical anion states of nucleobases in DNA
Alexander A. Voityuk, *Phys. Chem. Chem. Phys.*, 2009
DOI: 10.1039/b910690a

Effects of the biological backbone on DNA–protein stacking interactions
Cassandra D. M. Churchill, Lex Navarro-Whyte, Lesley R. Rutledge and Stacey D. Wetmore, *Phys. Chem. Chem. Phys.*, 2009
DOI: 10.1039/b910747a

The impact of monovalent ion force field model in nucleic acids simulations
Agnes Noy, Ignacio Soteras, F. Javier Luque and Modesto Orozco, *Phys. Chem. Chem. Phys.*, 2009
DOI: 10.1039/b912067j

Structural ultrafast dynamics of macromolecules: diffraction of free DNA and effect of hydration
Milo M. Lin, Dmitry Shorokhov and Ahmed H. Zewail, *Phys. Chem. Chem. Phys.*, 2009
DOI: 10.1039/b910794k

Simulation of DNA double-strand dissociation and formation during replica-exchange molecular dynamics simulations
Srinivasaraghavan Kannan and Martin Zacharias, *Phys. Chem. Chem. Phys.*, 2009
DOI: 10.1039/b910792b

Sensors for DNA detection: theoretical investigation of the conformational properties of immobilized single-strand DNA
Vincenzo Barone, Ivo Cacelli, Alessandro Ferretti, Susanna Monti and Giacomo Prampolini, *Phys. Chem. Chem. Phys.*, 2009
DOI: 10.1039/b914386f

Relaxation dynamics of nucleosomal DNA
Sergei Y. Ponomarev, Vakhtang Putkaradze and Thomas C. Bishop, *Phys. Chem. Chem. Phys.*, 2009
DOI: 10.1039/b910937b

Dynamics of a fluorophore attached to superhelical DNA: FCS experiments simulated by Brownian dynamics
Tomasz Wocjan, Jan Krieger, Oleg Krichevsky and Jörg Langowski, *Phys. Chem. Chem. Phys.*, 2009
DOI: 10.1039/b911857h

A detailed binding free energy study of 2 : 1 ligand–DNA complex formation by experiment and simulation
Witcha Treesuwan, Kitiyaporn Wittayanarakul, Nahoum G. Anthony, Guillaume Huchet, Hasan Alniss, Supa Hannongbua, Abedawn I. Khalaf, Colin J. Suckling, John A. Parkinson and Simon P. Mackay, *Phys. Chem. Chem. Phys.*, 2009
DOI: 10.1039/b910574c

Molecular simulation of conformational transitions in biomolecules using a combination of structure-based potential and empirical valence bond theory
Giuseppe de Marco and Péter Várnai, *Phys. Chem. Chem. Phys.*, 2009
DOI: 10.1039/b917109f

Dependence of A-RNA simulations on the choice of the force field and salt strength
Ivana Beššeová, Michal Otyepka, Kamila Réblová and Jiří Šponer, *Phys. Chem. Chem. Phys.*, 2009
DOI: 10.1039/b911169g

Protein–DNA binding specificity: a grid-enabled computational approach applied to single and multiple protein assemblies
Krystyna Zakrzewska, Benjamin Bouvier, Alexis Michon, Christophe Blanchet and Richard Lavery, *Phys. Chem. Chem. Phys.*, 2009
DOI: 10.1039/b910888m

Evaluation of molecular modelling methods to predict the sequence-selectivity of DNA minor groove binding ligands
Hao Wang and Charles A. Laughton, *Phys. Chem. Chem. Phys.*, 2009
DOI: 10.1039/b911702d

Mesoscale simulations of two nucleosome-repeat length oligonucleosomes
Tamar Schlick and Ognjen Perišić, *Phys. Chem. Chem. Phys.*, 2009
DOI: 10.1039/b918629h

On the parameterization of rigid base and basepair models of DNA from molecular dynamics simulations
F. Lankaš, O. Gonzalez, L. M. Heffler, G. Stoll, M. Moakher and J. H. Maddocks, *Phys. Chem. Chem. Phys.*, 2009
DOI: 10.1039/b919565n

Charge transfer equilibria of aqueous single stranded DNA
Marco D'Abramo, Massimiliano Aschi and Andrea Amadei, *Phys. Chem. Chem. Phys.*, 2009
DOI: 10.1039/b915312h

Relaxation dynamics of nucleosomal DNA†

Sergei Y. Ponomarev,‡*[a] Vakhtang Putkaradze*[b] and Thomas C. Bishop*[c]

Received 3rd June 2009, Accepted 27th August 2009
First published as an Advance Article on the web 21st September 2009
DOI: 10.1039/b910937b

Recent experimental and theoretical evidence demonstrates that proteins and water in the hydration layer can follow complex stretched exponential or power law relaxation dynamics. Here, we report on a 50 ns all atom molecular dynamics (MD) simulation of the yeast nucleosome, where the interactions between DNA, histones, surrounding water and ions are explicitly included. DNA interacts with the histone core in 14 locations, approximately every 10.4 base pairs. We demonstrate that all sites of interaction exhibit anomalously slow power law relaxation, extending up to 10 ns, while fast exponential relaxation dynamics of hundreds of picoseconds applies to DNA regions outside these locations. The appearance of $1/f^{\alpha}$ noise or pink noise in DNA dynamics is ubiquitous. For histone-bound nucleotide dynamics $\alpha \rightarrow 1$ and is a signature of complexity of the protein–DNA interactions. For control purposes two additional DNA simulations free of protein are conducted. Both utilize the same sequence of DNA, as found the in the nucleosome. In one simulation the initial conformation of the double helix is a straight B-form. In the other, the initial conformation is super helical. Neither of these simulations exhibits the variation of α as a function of position, the measure of power law for dynamical behavior, which we observe in the nucleosome simulation. The unique correspondence (high α to DNA–histone interaction sites, low α to free DNA sites), suggests that α may be an important and new quantification of protein–DNA interactions for future experiments.

1. Introduction

Relaxation in proteins happens over a wide range of times from sub-picoseconds to milliseconds or longer[1] and has been extensively studied by numerous experimental and theoretical groups.[2–9] Recently it was demonstrated that proteins and hydration water at protein surfaces follow complex stretched exponential[4,7] or power law relaxation dynamics.[2,3,5,10–12] These two forms of molecular relaxation were explained by the coexistence of multiple isoenergetic states in analogy to glasses.[13,14] There is strong evidence that both proteins and hydration water behave as amorphous, disordered systems and that their dynamics are coupled.[15–18] Indeed, water dynamics was shown to be significantly slowed down at protein surfaces.[19–21] The presence of $1/f^{\alpha}$ noise[22] with the same value of α in the potential energy fluctuations of protein and hydration water further supports the coupling hypothesis.[23–25] Nevertheless, it remains unclear whether power law relaxation is inherent to protein or hydration layer dynamics.

Intuitively, there should also be dynamical coupling between proteins and DNA in the bound state. Some spectroscopic evidence suggests that DNA dynamics in complexes with proteins or drugs is slowed down by a factor of two or higher.[9,26] Relaxation of free DNA in solution is observed on the picosecond to nanosecond time scale and has exponential form.[10,27–31] However, recent fluorescent experiments detected a 40 femtosecond to 40 nanosecond power law decay of the spectral signal for free DNA in solution.[12] This anomalously slow process was later attributed to water dynamics in the hydration layer[10] based on energy decomposition using MD simulation and a linear response approximation.[3] DNA in the nucleosome is ideal for investigating relaxation dynamics because the double helix is approximately one persistence length (50 nm) and there is a regular variation of protein–DNA contacts.

Nucleosomes, the elemental structural units of chromatin, effect DNA transcription, replication, and repair.[32–34] The nucleosome consists of 146 base pairs of double-stranded DNA wrapped in 1.7 left-handed super helical turns around an octameric histone core, (H2A·H2B)(H3·H4)$_2$(H2A·H2B). DNA interacts strongly with the histone core at 14 locations or approximately every 10.4 base pairs. The position of nucleosomes in chromatin is a key determinant of chromatin's gross structure. Variations in DNA sequence, conformation, and flexibility are essential elements in this positioning; however, less is known about the role of dynamics of DNA either within the nucleosome, the linker region, or between free and bound states of DNA. MD simulations are extremely useful for such studies. Recent advances in supercomputer power have made the simulations of

[a] *Tulane University, Center for Computational Science, Lindy Boggs Center Suite, 500 New Orleans, LA, 70118, USA. E-mail: sponomarev@wpi.edu*
[b] *Department of Mathematics, Colorado State University, Fort Collins, CO 80523, USA. E-mail: putkarad@math.colostate.edu*
[c] *Tulane University, Center for Computational Science, Lindy Boggs Center Suite, 500 New Orleans, LA, 70118, USA. E-mail: bishop@tulane.edu; Fax: +1 (504)862-8392; Tel: +1 (504)862-3370*

† Electronic supplementary information (ESI) available: Additional theoretical data. See DOI: 10.1039/b910937b

‡ Current address: Department of Chemistry and Biochemistry, Worcester Polytechnic Institute, Worcester, MA 01609, USA

nucleosomes possible.[35–39] Molecular dynamics simulations have shown that DNA in the nucleosome is less flexible than when free in solution,[37] and analysis of over 20 crystal structures indicates that nucleosomes require variations in the geometry of the DNA superhelix on two length scales: 10.4 and 146 base pairs.[40] However, relaxation dynamics inherent to nucleosomal or free DNA of persistence length have not yet been explored.

Here we report on DNA relaxation dynamics in a yeast nucleosome, PDB id: 1id3,[41] based on a 50 ns MD simulation, labeled nuc-1id3. For control purposes we compare this simulation to two reference 20 ns simulations of the same sequence where protein was not present. In one, the DNA is super coiled, as in the crystal structure, and is labeled sc-DNA. In the other, the DNA is initially straight and is labeled AB-DNA. The dynamics of the DNA is analyzed as a function of position along the double helix using the DNA inter-base pair helical parameters. This method is different from the conventional analysis of the potential energy fluctuations, often used in the literature.[3,10,18,27] Our method of analysis provides a more detailed and localized description of dynamics than what is typically considered. By focusing on DNA helical parameters our results can also be directly compared to geometrically exact elastic rod models, *e.g.* ref. 42 and 43, classical Kirchhoff theory,[44] or exact geometric theory with the effect of nonlocal interactions.[45,46]

2. Theory

For a dynamical system described by a scalar quantity $Y(t)$ we define its autocorrelation function as

$$C(\tau) = \int_0^\tau (Y(t) - \bar{Y})(Y(t+\tau) - \bar{Y})\,\mathrm{d}t \qquad (1)$$

where $\bar{Y}$ is the average of $Y(t)$ from 0 to τ. A relaxation time, τ_r, may be extracted from the autocorrelation by fitting to a single exponential function $C(\tau) \sim Ae^{-t/\tau_r}$. More general fitting procedures allow for multiple relaxation times or a stretched exponential $Ae^{(-t/\tau_r)\beta}$ as in the Kohlrausch–Williams–Watts function.[2,7,47,48] In all cases the relaxation time can be interpreted as a measure of the length of time it takes for the system to forget its former state.

One can also consider the spectral density function, $S(f)$, defined as the Fourier transform of $C(\tau)$ or $F[C](f) = S(f)$. In principle, $S(f)$ contains as much information as the auto-correlation function, and for idealized systems it does not make a difference whether one considers $C(\tau)$ or $S(f)$. However, in real systems the presence of noise, inaccurate data in some regimes, *etc.*, often make the consideration of the spectral density function advantageous. This is due to the fact that $S(f)$ describes combined dynamics on all time scales, available in the data set.

Some functional forms of $S(f)$ are particularly interesting. In the case $S(f) \propto 1/f^\alpha$, the system is said to exhibit $1/f^\alpha$, or power law noise and is often referred to as simply $1/f$ noise. We prefer the more detailed $1/f^\alpha$ noise notation. White noise corresponds to $\alpha = 0$, red noise to $\alpha = 2$, and pink noise is characterized by $0 < \alpha < 2$.

White noise is the foundation of stochastic theory and simply refers to a stochastic process, denoted $Y(t) = w(t)$, with no temporal correlation. The result at every time step $w(t_{n+1})$ is independent of the result of the previous time step $w(t_n)$. The power spectrum of white noise is flat, *i.e.*, $S(f) = \text{const}$. Physically, the probability of finding any harmonic in a white noise signal is equal for all harmonics.

Red noise is also known as Brown noise, Brownian noise or random walk noise. Brownian motion, denoted $Y(t) = b(t)$, stems from summing the results of a white noise process for individual steps. Naively, $b(t)$ comes from integrating the result of a white noise process, [EQUATION], so $S(f) \propto 1/f^2$. For more details and rigorous exposition of this theory we refer the reader to ref. 49.

Pink noise or flicker noise is intermediate between white and red. It is ubiquitous in nature, appearing in a wide range of complex systems such as, for example, music and speech,[50,51] heart rate,[52] semiconductors and carbon nanotubes,[53,54] environmental time series,[55] financial market fluctuations,[56] cosmic radiation,[57] DNA base sequences[58] and protein and hydration water dynamics.[2,23]

To explain our results, it is tempting to try to derive a simplified dynamical model, based on a finite system of springs forced by random noise, with the springs modeling the elastic interactions between the base pairs and the random noise modeling the interaction of DNA with solute or protein. Unfortunately, no such system can be derived to explain pink noise, no matter how simple or how complex that system may be. The reason is that such a simplified model must necessarily be of the form

$$\frac{\mathrm{d}^2}{\mathrm{d}t^2}\mathbf{Y} + \mathbf{L}\cdot\mathbf{Y} = \mathbf{w}, \qquad (2)$$

where $\mathbf{Y}(t)$ is a vector, describing deformation of each site, and $\mathbf{L}$ is an antisymmetric matrix, representing the vector of elastic response and coupling. More precisely, the element $L_{ij} = -L_{ji}$ of the matrix $\mathbf{L}$ corresponds to the elastic constant for the coupling between components i and j at each site. The forcing function is $\mathbf{w}$ and arises from interactions with solute or protein, with each w_i assumed to be white noise. Treating the right hand side (somewhat loosely), as the external forcing of the DNA, we see that the Fourier transform of eqn (2) satisfies

$$F[\mathbf{Y}] = (\mathbf{L} - f^2\mathbf{I})^{-1}F[\mathbf{w}], \qquad (3)$$

where $\mathbf{I}$ is the identity matrix. Note that since $\mathbf{w}$ is assumed to be white noise, $F[\mathbf{w}]$ is constant.

The resolvent $(\mathbf{L} - f^2\mathbf{I})^{-1}$ has a simple pole in f^2 whenever f^2 approaches λ, an eigenvalue of $\mathbf{L}$. Thus, the resolvent $(\mathbf{L} - f^2\mathbf{I})^{-1}$ has only simple poles that are of the type

$$(\mathbf{L} - f^2\mathbf{I})^{-1} \sim (f - \sqrt{\lambda})^{-1}(f + \sqrt{\lambda})^{-1}$$

when $\lambda > 0$ and

$$(\mathbf{L} - f^2\mathbf{I})^{-1} \sim (f^2 + |\lambda|)^{-1}$$

for $\lambda < 0$.

Since for physical reasons $F[Y]$ has to decay to zero as $f \to \infty$, the rational fraction expansion of $F[Y]$ in terms of inverse powers of f cannot contain a constant term. It must start with, at least, $F[Y] \sim 1/(f - f_0)^p$, with $p \geq 1$ being an

integer number. On the other hand, since $S(f) = |F[Y]|^2$, then $S(f) \sim 1/(f - f_0)^{2p}$, or (in our notation) $\alpha \geq 2$. Therefore, pink noise would require fractional powers expansion of the resolvent which is clearly impossible in the framework of this simple mechanical model.

The exact nature of the signal $\mathbf{Y}(t)$ will, of course, depend on the properties of the coupling matrix $\mathbf{L}$. In any case, $1/f$ noise and pink noise in general cannot be explained in terms of a simple physical model and more complex considerations are warranted. One of the explanations of general $1/f$ noise has been the existence of the so-called critical states, the minimally stable self-organized states originating from dynamical processes.[59]

This agrees with our discussion in the Introduction, where we mentioned the presence of $1/f^{\alpha}$ noise with the same value of α in the potential energy fluctuations of protein and hydration water.[22–25] Clearly, these results support the coupling hypothesis. However, it remains unclear whether power law relaxation is inherent to the protein or to the hydration water. For DNA, pink noise was observed in temperature fluctuations, obtained from a non-atomic model.[60] In that work, power law fluctuations arise from the consideration of a large number of base pairs and not from the dynamics of a single base pair.

In the remainder of this paper we will not consider the theoretical origins of pink noise, but rather show that pink noise is present in the helical parameters of DNA for all our simulations, whether the DNA is bound to protein or free in solution. Only in the case of nuc-1id3, the nucleosome simulation, is there a regular variation of α as a function of position along the DNA. Thus, the key result is that the α-parameter is weakly affected by DNA conformation but is strongly affected by DNA–protein contacts.

3. Methods

Simulation techniques

A molecular dynamics simulation of yeast nucleosome,[41] PDB id: 1id3, was performed in NAMD[61] using the parm99 force field[62] of AMBER[63] together with the parmbsc0 refinement.[64] This simulation is labeled nuc-1id3. The 3.1 Å resolution X-ray structure included a histone octamer (H2A·H2B)(H3·H4)$_2$(H2A·H2B), a palindromic DNA fragment of 146 base pairs, 17 Mn^{2+}, and 60 water molecules. The waters and manganese ions were removed when building the system. Instead, 217 neutralizing Na^+ ions were added with the addions command in tleap, followed by addition of a 12 Å TIP3P solvent layer. Subsequently, 109 excess NaCl ion pairs were added to create a physiological concentration of 150 mM. Sodium parameters of Aqvist[65] and chlorine parameters of Fox[66] were adopted. The final system contained 155 473 atoms (133 266 water, 12 492 protein, 9281 DNA, 326 Na^+ and 109 Cl^-) with zero net charge inside a system unit cell of $137 \times 101 \times 136$ Å^3. The system was minimized and equilibrated using the protocol developed by Bishop[37] for simulating nucleosomes. After equilibration, 50 ns of NTP dynamics were computed using Louisiana Optical Network Initiative (LONI) resources. Half a nanosecond simulation took ~9 h on a 32 CPU Dell cluster with 2.33 GHz Intel Xeon 64 bit processors. Thus, a total of 28 800 CPU hours were required to complete this simulation. Two additional simulations of the same sequence of DNA free in solution, sc-DNA and AB-DNA, followed a similar protocol and were each performed for 20 ns, 4 times longer than the necessary MD sampling requirement of 5 ns.[28] Simulation sc-DNA, in which the DNA was super coiled, had the same starting structure as nuc-1id3 with an initial unit cell of $135 \times 84 \times 134$ Å and contained 127 139 atoms. Simulation AB-DNA, in which DNA was initially straight, was generated with the rebuild module of 3DNA[67] using Arnott B-DNA values.[68] The starting structure had initial unit cell size of $52 \times 52 \times 499$ Å^3 and consisted of a total of 98 301 atoms.

Data extraction

DNA helix parameters characterize DNA structure in terms of the internal coordinates of the base pairs.[69,70] The six inter-base pair helix parameters include shift, slide and rise, which describe translational motions, and tilt, roll and twist, which describe rotations of the base pairs with respect to each other. Time series of helix parameters were obtained by running CURVES6[71] on consecutive snapshots extracted from trajectory files every $\Delta\tau = 10$ ps yielding a total of $N = 5000$ snapshots for the 50 ns simulation of nuc-1id3, and 2000 snapshots for each of the 20 ns simulations, sc-DNA and AB-DNA. The snapshot separation was chosen in such a way that the resulting trajectories were smooth, but not so small that extraneous data needed to be processed. In our simulations, $\Delta\tau = 10$ ps was a reasonable separation time between snapshots satisfying both of these requirements.

Root mean square deviation is a measure of a conformational difference between two molecular structures and is calculated *via* the following formula:

$$\mathrm{RMSD} = \sqrt{\frac{1}{N}\sum_{i=1}^{N}(x_{2i} - x_{1i})^2 + (y_{2i} - y_{1i})^2 + (z_{2i} - z_{1i})^2}, \quad (4)$$

where N is the number of pairs of equivalent atoms and (x_{1i},y_{1i},z_{1i}), (x_{2i},y_{2i},z_{2i}) are the coordinates of the ith pair of equivalent atoms. In all RMSD calculations each set of equivalent atoms were fit to the set obtained for $t = 0$ before determination of the RMSD. For the 50 ns simulation of nuc-1id3, RMSD time series were also obtained for each of the 765 protein residues and for each base in the DNA using the same 10 ps sampling interval.

DNA B-factors for nuc-1id3, sc-DNA and AB-DNA were calculated using the "ptraj" module of AMBER with a time step of 0.5 ps. X-ray B-factors were obtained from the original pdb structure of the nucleosome. This data is included in the ESI†—see Fig. S5.

The protein contact map in Fig. 3 was obtained from protein occupancy data (see Fig. S10 of the ESI†). Occupancies were calculated from the 50 ns trajectory with a time step of 25 ps *via* the proximity analysis method[72] using a cutoff of 3.4 Å from DNA atoms. Occupancies below 10% of the maximum value in the dataset were assigned a score of

0 (free), while all others were given a score of 1 (bound). The exact percentage value used to convert from occupancy data to a binary contact map does not significantly affect the contact map (see Fig. S10†).

Data analysis

Autocorrelation functions of the DNA helix parameters were calculated for all 145 DNA inter-base pair steps. Autocorrelation functions of the RMSD time series were calculated for all 765 protein residues and all 292 DNA bases. The autocorrelation function for a discrete time series data was adopted from National Institute of Standards and Technology website[73] in the following form:

$$C(\tau) = \frac{\sum_{t=1}^{n-\tau} (Y_t - \bar{Y})(Y_{t+\tau} - \bar{Y})}{\sum_{t=1}^{N} (Y_t - \bar{Y})^2}, \qquad (5)$$

where t is simulation time, τ—lag time, n—number of data points, Y_t—values of either DNA helix parameters (shift, slide, rise, tilt, roll or twist) or protein RMSD at time t, and $\bar{Y}$—average values of helix parameters or protein RMSD. Note that eqn (5) is the (normalized) version of definition (1) for discrete sampling. A total of 870 DNA autocorrelation functions were calculated for each simulation, consisting of 6 helix parameters measured at 145 inter-base pair steps. A total of 765 protein autocorrelation functions were obtained for the nuc-1id3 simulation. Autocorrelations are plotted as three-dimensional graphs of $C_i(\tau)$ *versus* τ and i, where i denotes base pair step or residue index. An average autocorrelation function for each base pair step, denoted $\langle C_i(\tau)\rangle$ was also computed by combining the six values of $C_i(\tau)$.

Power spectral density distributions, $S(f)$, were obtained in Mathematica 6[74] from Discrete Fourier Transforms (DFT) of the autocorrelation functions $C(\tau)$ *via* the expression:

$$S(f) = \sum_{k=0}^{N} C(k\Delta\tau) e^{-\frac{2\pi i}{N} fk}, \qquad (6)$$

where f is the discrete frequency. Since our number of data points $N = 5000$ is not a power of 2, Fast Fourier Transform algorithms (FFT) cannot be used, but even in this relatively slow DFT setting data processing does not take substantial time. For the ith inter-base pair step, six $S_i(f)$ distributions were calculated from the correlation functions of shift, slide, rise, tilt, roll and twist. An average power distribution spectra, $\langle S_i(f)\rangle$, was then computed by combining the six values of $S_i(f)$ at each base pair step. Values of α_i were computed from the averaged DNA power spectra by linear fitting to doubly logarithmic plots of $\langle S_i(f)\rangle$. This procedure was also used to obtain α_i values from protein and DNA RMSD data. Note that in Fig. 3, the spectrum of α is plotted *versus* wavenumber, k, rather than frequency, f.

Finally, to determine the statistical significance of our results, a two sample paired t-test statistic was utilized. These calculations were performed in Origin 7.5.[75]

4. Results

The starting structures of nuc-1id3, sc-DNA and AB-DNA are represented in Fig. 1. During the course of the simulation DNA conformation stayed close to the B-form in all three molecular systems. This conclusion was based on our inspection of DNA helix parameters and sugar pucker conformations. Root mean square deviation values of DNA for nuc-1id3, sc-DNA and AB-DNA were calculated with respect to the corresponding starting structures (see Fig. S9 of the ESI†). Nucleosome simulation, nuc-1id3, was stable with average RMSD value of 4 Å. This result agrees well with other molecular dynamics simulations of nucleosomes.[37,40] Molecular structures of DNA in AB-DNA and sc-DNA deviated significantly from their starting conformations, showing maximum RMSD of 20 Å in each simulation. Since RMSD is a measure of conformational variation in Cartesian coordinates, such results were expected because of the extended length of the double helix in the first case and a tendency of the supercoiling to unwind in the second case. The RMSD values observed for AB-DNA agree well with a model that describes thermal fluctuations of 150 base pairs of DNA about its equilibrium conformation.[76] We further emphasize that our simulations of free DNA represent the limit of what can be reasonably achieved with currently available hardware and software resources. Ideally, the straight DNA simulation, AB-DNA, requires an octahedral box of $500 \times 500 \times 500$ Å^3. This is $\approx$66 times bigger than the nuc-1id3 simulation box, $137 \times 101 \times 136$ Å^3. The super coiled DNA simulation, sc-DNA, represents a non-equilibrium initial conformation in which the histones were simply replaced with solvent. It would require an undetermined amount of simulation time to unwind, and the simulation cell would have to be, at least, $500 \times 500 \times 500$ Å^3 to accommodate such a structural transition.

Given the above limitations we focus on the local dynamics of DNA as described by the time evolution of the inter-base pair helix parameters. These descriptors appear to have converged by 10 ns (autocorrelation functions for sc-DNA and AB-DNA tend to zero by 1 ns, as shown in Fig. 2).

Cross sections of the autocorrelation functions, $\langle C_i(\tau)\rangle$, obtained from helix parameter sets for nuc-1id3, sc-DNA and AB-DNA at time instances τ = 10 ps, 100 ps, 1 ns, 10 ns are represented in Fig. 2.§ Autocorrelation functions for nuc-1id3 exhibit a 10.4 base pair variation along the DNA length, corresponding to a full turn of the double helix. This variation is not present in the autocorrelation data from either sc-DNA or AB-DNA, see bottom plot of Fig. 3. While some autocorrelation functions in nuc-1id3 do not decay to zero even at 10 ns, others decay rapidly within hundreds of picoseconds (see Fig. 2 and 4 and Fig. S4†). This is not the case for sc-DNA and AB-DNA, where all $C_i(t)$ amplitudes drop dramatically by 1 ns (see Fig. 2 and Fig. S4†). Thus, while DNA conformation has a limited effect on dynamics, as demonstrated by the similarity of results obtained for sc-DNA and AB-DNA (see Fig. 2, the middle plot of Fig. 3, and Fig. S4†) the histone-DNA contacts, present only in nuc-1id3, drastically change DNA dynamics.

In Fig. 4, we demonstrate the difference between two dynamical regimes, by showing the behaviors of helical

§ We also present supplementary Fig. S1–S10† for complete data representation.

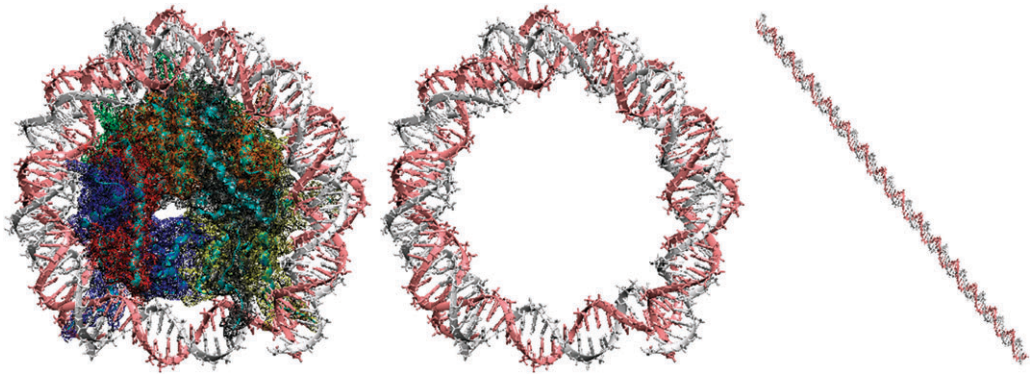

Fig. 1 Starting structures of nuc-1id3 (left), sc-DNA (middle) and AB-DNA (right), solvent not shown. Complementary strands are represented in white and pink, protein chains—in cyan, protein subunits—in mesh black, red, blue, yellow, orange, grey, green and white. sc-DNA and nuc-1id3 are on the same scale; AB-DNA is not.

parameters, associated with two different locations in the DNA. One location is inter-base pair step number 73 (step 0, as measured relative to the dyad). This step is in the middle of a region that lacks significant contact with protein, see Fig. 3. The data for this location is plotted in the left column of Fig. 4. The other location is inter-base pair step 68 (step-5, relative to the dyad) which is in contact with the protein and exhibits $\alpha \rightarrow 1$. This data is plotted in the right column of Fig. 4. The graphs in the left column of Fig. 4 describe fast relaxation dynamics, typical of a non-bound site, and correspond to motion that is rather close to white noise, $\alpha \rightarrow 0$. In terms of autocorrelation functions, $C(\tau)$, such motion is manifested by a fast exponential decay. In the spectral representation, *i.e.*, $S(f)$ and $\langle S(f)\rangle$ (middle and bottom plots), α corresponds to the slope of the data. We observe a wide variation in α and, therefore, rough $1/f^{\alpha}$ motion, with α being very small and deviations from a simple power law behavior being large. The graphs in the right column of Fig. 4 represent the dynamics of a typical site in contact with protein. This form of dynamics is characterized by a slow decay of the autocorrelation functions, $C(\tau)$. In the spectral domain (middle and bottom plots) we see a much better defined $1/f^{\alpha}$ signal with $\alpha \rightarrow 1$, and the deviations from the pink noise being small. We remark that the data obtained by averaging over all six helical parameters, $\langle S(f)\rangle$ is to be considered particularly well defined for this type of analysis.

Our key result is presented in Fig. 3: the α-parameter is weakly affected by DNA conformation but strongly affected by DNA–protein contacts. We refer to such data as an α *distribution* for brevity. Distributions of α for all three simulations are superimposed on the protein contact map, calculated from nuc-1id3. The protein contact map has 14 distinct peaks in agreement with 14 points of contact between protein and DNA observed, for example, in the 2.8 Å crystal structure of the nucleosome (PDB id 1AOI).[77] In our simulation, interaction sites were determined from the protein occupancy data, a distance based method (see methods section for details). The range of α for sc-DNA is 0.24 to 0.89, with $\langle\alpha\rangle = 0.59$; for AB-DNA $0.19 < \alpha < 0.78$ with $\langle\alpha\rangle = 0.55$; and for nuc-1id3 $0.17 < \alpha < 0.98$ with $\langle\alpha\rangle = 0.67$ (see Fig. 3). Note that in sc-DNA and AB-DNA frequency counts for $\alpha < 0.4$ or $\alpha > 0.8$ are significantly less than in nuc-1id3, indicating that protein–DNA contacts in nuc-1id3 have altered the α distribution.

Surprisingly, the α distributions for sc-DNA and AB-DNA are well correlated to each other, suggesting that sequence rather than conformation dominates the dynamics of free DNA, at least, as determined by α-parameter analysis. This correlation is present on all length scales, except for $k = 13$ (11.2 base pair) and $k = 16$ (9.1 base pair), as can be seen from Fig. 3 (bottom) which represents the power spectra of Fig. 3 (middle). It is tempting to interprete the peak at $k = 13$ for sc-DNA as a conformational effect. If this is in fact the case, then the peak shifted from $k = 14$ (10.4 base pair), as observed in nuc-1id3, to $k = 13$ (11.2 base pair). This is consistent with a tendency of DNA to unwrap and straighten in sc-DNA, whereas the highly bent superhelix conformation is maintained in nuc-1id3 by the presence of the histones.

In the case of nuc-1id3, the nucleosomal simulation, we observe the following: variations of α exhibit a strong periodicity, correlate with protein occupancy data, and tend to approach 1 for the bound regions. The observed periodicity is shown in Fig. 3 (bottom) by the peak at wavenumber $k = 14$, corresponding to $146/14 = 10.4$ base pair. Our results clearly indicate that, in the nucleosome, $\alpha \rightarrow 1$ for DNA regions in contact with histones while for DNA regions not contacting histones α tends to values associated with free DNA.

Secondary peaks at $k = 1$ (146 base pair) and 2 (73 base pair) in Fig. 3 (bottom) characterize the dynamics of the nucleosome but not free DNA, *i.e.* sc-DNA or AB-DNA. These wave numbers were identified as being both necessary and sufficient for obtaining superhelix geometry.[40] Such long length scale variations were also identified in ref. 37 in association with the dynamics of nucleosomal DNA. All three simulations share peaks at $k = 19$ (7.7 base pair) and $k = 11$ (13.3 base pair). These peaks could be a signature of this particular sequence of DNA.

To confirm that the observed variation in α is due to contact between protein and DNA rather than conformation of DNA we present Fig. 5. This figure shows the results from α-parameter analysis of RMSD values for individual DNA bases rather than inter-base pair steps (left), for protein residues (middle) and for the combined nucleosome structure (right). All images represent results from simulation nuc-1id3;

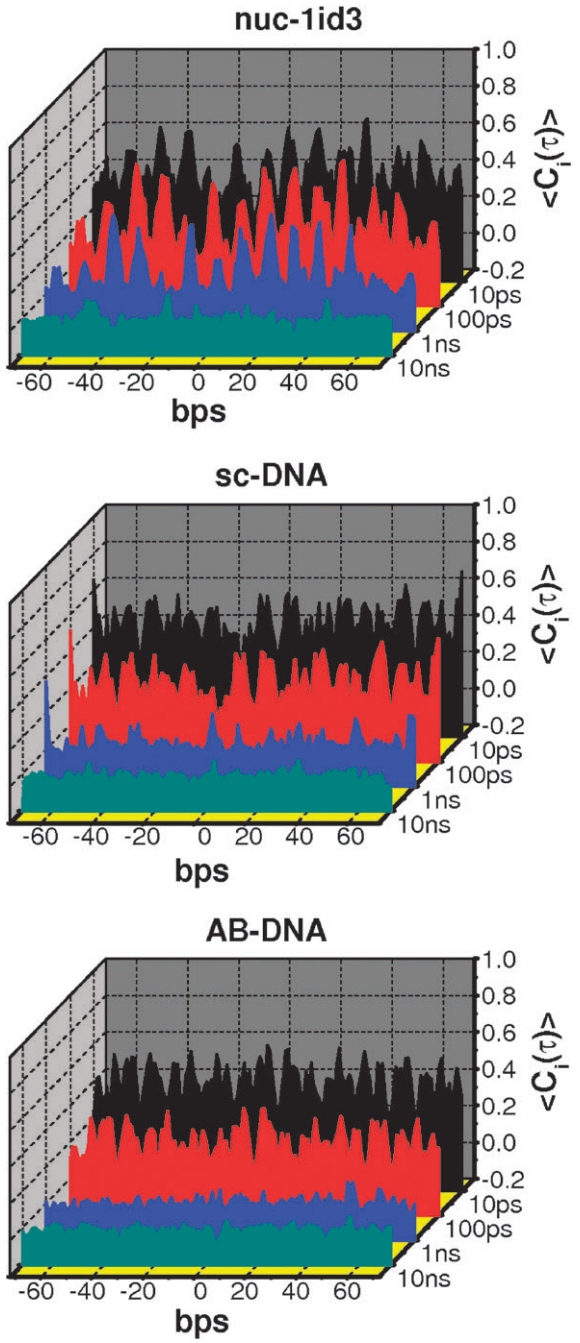

Fig. 2 Cross sections of 3D autocorrelation functions, $\langle C_i(\tau)\rangle$, for helix parameter data from simulations nuc-1id3 (top), sc-DNA (middle) and AB-DNA (bottom) *versus* base pair step, *i*, at times τ = 10 ps, 100 ps, 1 ns, 10 ns. $\langle C_i(\tau)\rangle$ is an average of the autocorrelation for shift, slide, rise, tilt, roll and twist, calculated at time τ and position *i*, see Methods for details.

the separation of DNA and protein is only for illustration purposes. The color-coding is such that blue corresponds to high values of α, red corresponds to low values of α, and white to intermediate values. Inspection of the images in Fig. 5 indicates that, except for end effects, DNA appears blue whenever there is a strong contact between protein and DNA and white or red elsewhere. For some base pairs, only the base in contact with protein appears blue, while the base exposed to solvent appears red. These details cannot be captured by α-parameter analysis of DNA helical parameters because the latter are base *pair* data rather than individual base specific data.

5. Discussion

There is a significant contribution from $\alpha > 0.8$ in the α-distribution for nucleosomal DNA. This contribution is absent in the α-distributions for free DNA, see Fig. 3 (top). Physically, the α-parameter characterizes the complexity of a relaxation process. Thus, protein contacts, which are present only in the nucleosome simulation, introduce dynamic complexity into nucleosomal DNA that does not exist in free DNA.

Proteins exhibit complex dynamics—their energy landscapes have many local minima. In contrast, the relaxation dynamics of bulk water is a simple, fast exponential process characterized by relaxation times of a few picoseconds.[26,78] Values of $\alpha \approx 1$ are indicators of a multi-relaxation dynamics, as observed in proteins. For values of α near zero, deviations from power law behavior increase and relaxation is more accurately described by a simple, fast exponential process, as observed for liquids. The 10.4 base pair variation ($k = 14$) in α, found only in our nucleosome simulation, nuc-1id3, agrees with this interpretation. The DNA varies between strong protein contacts and solvent exposure with every turn of the double helix.

Power law behavior with $\alpha \approx 1$ was reported previously for the dynamics of plastocyanin protein and hydration water, indicative of a possible surface effect.[2,24] In contrast to these findings a value of $\alpha = 0.7$ was detected for the solvation layer dynamics of native-state α-lactalbumin,[5] while the bulk water dynamics corresponded to $\alpha = 0.9$. The authors mention that a value of $\alpha < 1$ is a signature of anomalous diffusion of water molecules at protein's surface. Another study of relaxation dynamics in liquid water revealed collective motions and fluctuations characterized by multiple relaxation processes and $1/f^{\alpha}$ type of power spectra, also observed in water clusters.[79] The authors report a value of $\alpha = 0.75$ for the 64 water molecule MD simulation. The physical picture they presented—formation of random water clusters—is in agreement with the explanation of power law noise provided by Bak–Tang–Wiesenfeld models.[59,80,81] While it is possible that similar mechanisms are at play here, large systems tend to possess some physical quantities such as dielectric relaxation and the individual dipole relaxation which are exponential in nature. Thus, the dynamics discussed here may be a competition between exponential and power law behavior.

High values of α, *i.e.*, $\alpha \simeq 1$ appear whenever DNA contacts protein, as can be seen from Fig. 3 (middle). Values of α for free DNA in solution and for the water-exposed regions of the nucleosomal DNA approach white noise ($\alpha = 0$) which is characteristic of a stochastic system with no temporal correlation. Thus, low values of α possibly correspond to the short memory of the interactions between water molecules and DNA, and, also, to the stochasticity of water dynamics. Fast exponential decay of autocorrelation functions within few hundreds of picoseconds of the simulation time characterizes this form of relaxation mechanism. Our observation of $1/f^{\alpha}$ noise in the

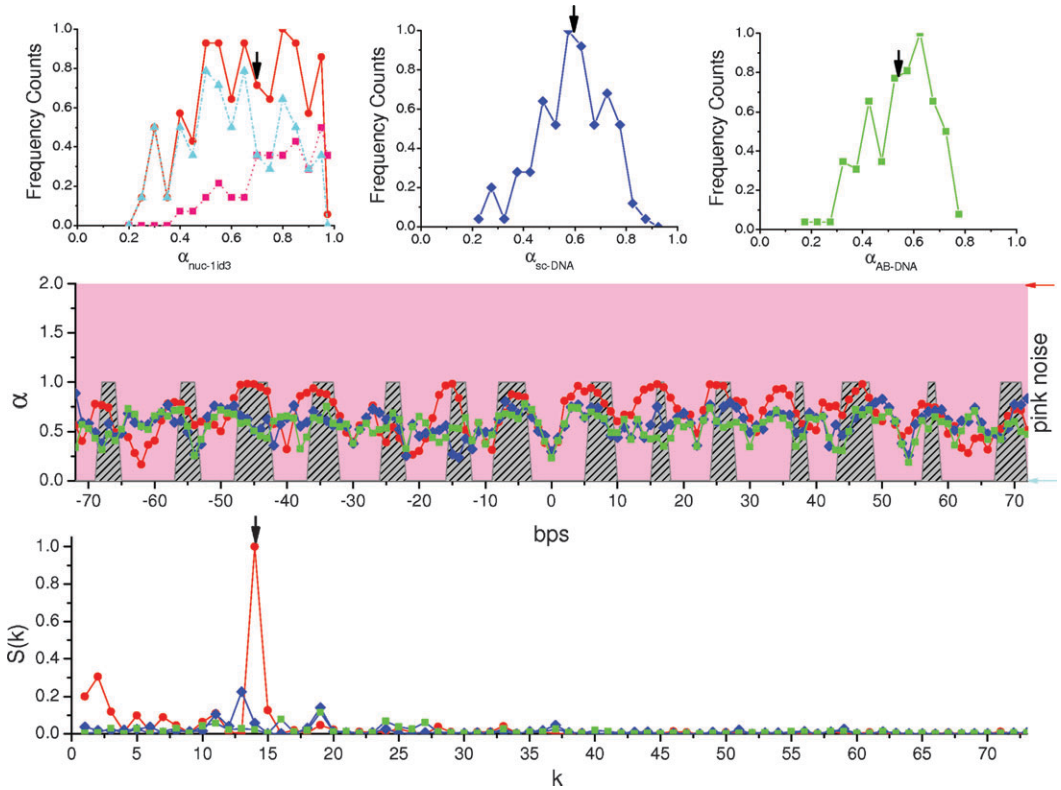

Fig. 3 **Top**: Normalized frequency counts of α for nuc-1id3 (left), sc-DNA (middle) and AB-DNA (right). Cyan triangles and pink squares (left) show frequency counts for free and bound DNA regions, respectively. **Middle**: Values of α for nuc-1id3 (red circles), sc-DNA (blue rhombuses) and AB-DNA (green squares) and protein contact map of nuc-1id3 (grey dashed lines) *versus* DNA inter-base pair step. **Bottom**: Power spectra of α. Arrows indicate average values of α in the top plots; limits of red noise and white noise in the middle plots, and the dominate peak at $k = 14$ for nuc-1id3 in the bottom plot.

power spectral densities of DNA and protein dynamics (see Fig. 5) suggests that there is dynamical coupling between protein and DNA at interaction sites.

We do not expect all sites of interaction to exhibit the same values of α. Different interaction sites will have slightly different amplitudes of their autocorrelation functions due to differences in protein occupancies, DNA and protein sequences and, to a lesser degree, conformations of the DNA or the protein at interaction locations. Thus, the value of α should vary with the details of the interaction.

To further support this conclusion we provide Table 1, showing α statistics for nuc-1id3, sc-DNA and AB-DNA. In nuc-1id3, the bound DNA regions exhibit an average value of α of 0.78 ± 0.16, while for the unbound regions the average is 0.61 ± 0.20. The latter is nearly identical to the average values obtained in sc-DNA (0.59 ± 0.14) and AB-DNA (0.55 ± 0.13).

We also performed two sample paired *t*-tests for the distributions of α shown in Fig. 3(top). Populations of α for free and bound regions of the nucleosomal DNA appear to be significantly different at the 0.05 level of confidence, free/bound ($t = 2.91$, $P = 0.01$). This result suggests that α values can be used to characterize the two different types of dynamic behavior shown in Fig. 4. Populations of α for sc-DNA and AB-DNA were found to be significantly different from that of nuc-1id3 at the 0.05 level of confidence, nuc-1id3/sc-DNA ($t = 3.37$, $P = 0.00$), nuc-1id3/AB-DNA ($t = 2.99$, $P = 0.00$). In contrast, the populations of α for sc-DNA and AB-DNA were found to be not significantly different at the 0.05 level, sc-DNA/AB-DNA ($t = 0.26$, $P = 0.80$). In the statistical data, provided above, *t* is the test statistic, used to evaluate the null hypothesis, and, *P* is the probability of obtaining a test statistic as extreme or more extreme than *t* due to chance factors alone. Thus, it is possible to distinguish between α populations for nucleosomal and free DNA, whether super coiled or straight, with a confidence level of 0.05. The effects, arising directly from protein–DNA interactions, are also shown in Fig. S6 and S7 of the ESI† which present cross sections of 3D differential autocorrelation functions for nuc-1id3 (cross sections for free DNA were subtracted from cross sections for nucleosomal DNA). Thus, it is clear that protein effects exist, and the average value of α in nuc-1id3 is higher compared to the other two simulations because of protein coupling.

Hence, we associate high values of α to protein–DNA coupling and low values of α to water diffusion at DNA surface. We argue that long temporal correlation of the signal (of up to 10 ns) detected for the bound DNA bases is due to the effect of a highly deterministic system, the protein. Short temporal correlation (of hundreds of picoseconds) for the water-exposed DNA bases has to be associated with water diffusion at DNA surface and is a stochastic process. This would explain why $1/f^{\alpha}$ noise becomes pinker (large α) for the bound states and whiter (small α) for the states exposed to water. This is illustrated in Fig. 5, where we color-code the

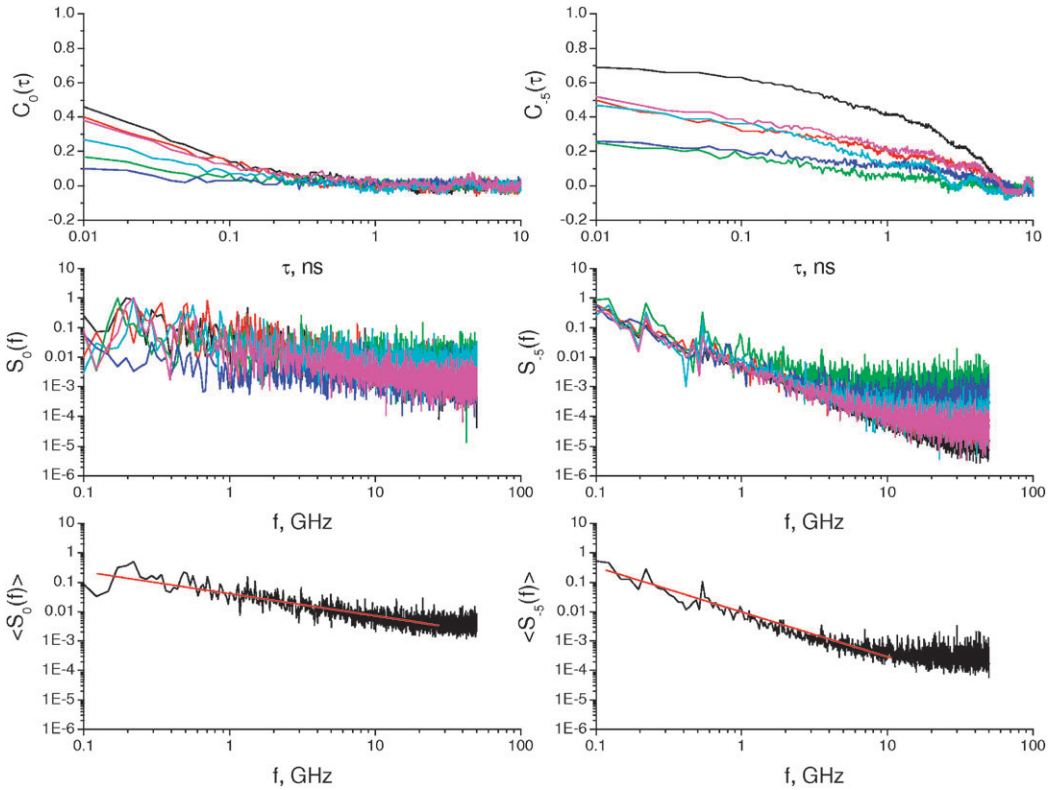

Fig. 4 Analysis of a water exposed region, step 0 relative to dyad (left column), and a region in contact with histones, step -5 relative to dyad (right column), from simulation nuc-1id3. **Top**: autocorrelation functions, $C_i(\tau)$. **Middle**: the corresponding power spectral densities, $S_i(f)$. Black curves represent shift, red-slide, green-rise, blue-tilt, cyan-roll and magenta-twist. **Bottom**: power spectral densities, $\langle S_i(f)\rangle$. Red lines represent fits to $\langle S_i(f)\rangle$ data with $\alpha = 0.39$, $R^2 = 0.56$ (left) and $\alpha = 0.87$, $R^2 = 0.96$ (right).

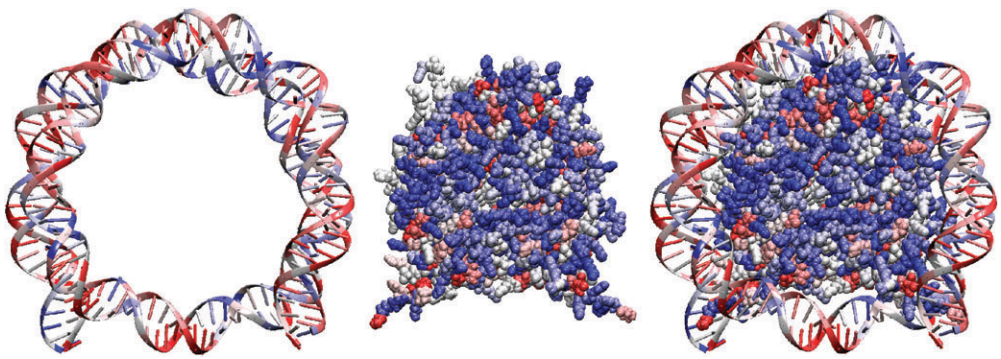

Fig. 5 DNA (left), protein (middle) and nucleosome (right) structures from simulation nuc-1id3 color-coded by α. Red corresponds to $\alpha = 0$, white to $\alpha = 0.5$, blue to $\alpha = 1$.

Table 1 Statistics on α-exponents for nuc-1id3, sc-DNA and AB-DNA. $\langle\alpha\rangle$ represents the average over all base steps. $\langle\alpha_{bnd}\rangle$ is the average over only the base pair steps in contact with protein as indicated in Fig. 3 and $\langle\alpha_{free}\rangle$ is the average over steps that are not contacting protein

Parameter	nuc-1id3	sc-DNA	AB-DNA
$\langle\alpha\rangle \pm$ sd	0.67 ± 0.20	0.59 ± 0.14	0.55 ± 0.13
$\langle\alpha_{bnd}\rangle \pm$ sd	0.78 ± 0.16	N/A	N/A
$\langle\alpha_{free}\rangle \pm$ sd	0.61 ± 0.20	N/A	N/A

average nucleosome structure by the value of α at each site. A regular pattern of blue, corresponding to $\alpha \approx 1$, on the inside of the DNA is observed for regions of contact. Interestingly, the outer protein surface, formed largely by charged and polar amino acid residues, is also dominated by the blue color. This, once again, suggests that complex power law dynamics, observed in DNA, is inherent to that of the histone core.

We propose that the presence of $1/f^{\alpha}$ power law relaxation with $\alpha \approx 1$ in the dynamics of nucleosomal DNA is a manifestation of DNA–histone interaction. We associate this phenomena with complex DNA dynamics on multiple time scales, ranging from picoseconds to tens of nanoseconds. Simple exponential models do not apply in this case. This form of dynamics has a characteristic power law spectra, commonly observed in proteins. Dynamics outside interaction

sites is comparable to that of free DNA, exposed to water. Thus, we believe that there is an important connection between protein or solvent contact and the distribution of α values as descriptors of the dynamics of DNA. As far as we are aware, we are the first to make this interesting connection.

6. Conclusion

We analyzed DNA relaxation dynamics of nucleosomal DNA and of DNA free in solution (super coiled and straight). A power law approximation was used to describe the relaxation process. Pink noise, $1/f^{\alpha}$ with $0 < \alpha < 2$, was present in the dynamics of all base pairs in all systems; however, the best fits were obtained for DNA regions interacting with the histone octamer in the nucleosome. We were, thus, able to classify DNA dynamics as: (a) fast exponential relaxation of hundreds of picoseconds for DNA regions exposed to water and (b) slow power law relaxation of more than 1 ns for DNA regions in contact with the histones. For DNA in the nucleosome, pink noise ($1/f^{\alpha}$ with $\alpha \rightarrow 1$) was observed every 10.4 base pairs and was associated with protein–DNA contact. No such variation in α as a function of position existed for DNA free in solution, whether it was straight or super coiled. Between sites of protein–DNA contact, nucleosomal DNA has dynamic properties similar to those of free DNA in solution. Protein free regions exhibited fast exponential decay of autocorrelation functions and $1/f^{\alpha}$ noise with average $\alpha = 0.6$. These observations supported the hypothesis that protein fluctuations dominated DNA motions at interaction sites. Furthermore, we found that variation of dynamics as a function of position for super coiled, but otherwise free DNA, was correlated to that of straight DNA. Thus, DNA conformation played a minor role in dynamics as determined by α-parameter analysis.

In summary, nucleosomal DNA can be distinguished from free DNA not only by conformation but also by its dynamic signature. We expect that non-histone DNA binding proteins, which are sensitive to both DNA conformation and dynamics, can therefore discriminate between straight DNA, super coiled DNA, bent DNA, and nucleosomal DNA. Discriminating between various DNA geometries requires only sensitivity to conformation, *e.g.*, bend recognition. Discriminating between bound and free DNA requires sensitivity to dynamics. We suggest that this type of dynamic signature plays an important role in DNA recognition and that our α-parameter analysis is a metric for describing it.

Acknowledgements

Portions of this research were conducted with high performance computational resources provided by the Louisiana Optical Network Initiative (http://www.loni.org). T. C. Bishop and S. Y. Ponomarev received support for this work by NIH grant R01GM076356 and the Louisiana Board of Regents Research Competitiveness Program contract LEQSF 2005-08-RD-A-34.

References

1 R. M. Levy, J. A. Karplus and M. McCammon, Molecular Dynamics Studies of NMR Relaxation in Proteins, *Biophys. J.*, 1980, **32**(1), 628–630.
2 A. Bizzarri and S. Cannistraro, Molecular Dynamics of Water at the Protein-Solvent Interface, *J. Phys. Chem. B*, 2002, **106**, 6617–6633.
3 L. Nilsson and B. Halle, Molecular origin of time-dependent fluorescence shifts in proteins, *Proc. Natl. Acad. Sci. U. S. A.*, 2005, **102**, 13867–13872, DOI: 10.1073/pnas.0504181102.
4 A. A. Golosov and M. Karplus, Probing polar solvation dynamics in proteins: a molecular dynamics simulation analysis, *J. Phys. Chem. B*, 2007, **111**, 1482–1490, DOI: 10.1021/jp065493u.
5 N. Sengupta, S. Jaud and D. J. Tobias, Hydration dynamics in a partially denatured ensemble of the globular protein human alpha-lactalbumin investigated with molecular dynamics simulations, *Biophys. J.*, 2008, **95**, 5257–5267, DOI: 10.1529/biophysj.108.136531.
6 M. Marchi, F. Sterpone and M. Ceccarelli, Water rotational relaxation and diffusion in hydrated lysozyme, *J. Am. Chem. Soc.*, 2002, **124**, 6787–6791.
7 R. Abseher, H. Schreiber and O. Steinhauser, The influence of a protein on water dynamics in its vicinity investigated by molecular dynamics simulation, *Proteins: Struct., Funct., Genet.*, 1996, **25**, 366–378.
8 S. Sen, N. A. Paraggio, L. A. Gearheart, E. E. Connor, A. Issa, R. S. Coleman, D. M. Wilson, M. D. Wyatt and M. A. Berg, Effect of protein binding on ultrafast DNA dynamics: characterization of a DNA:APE1 complex, *Biophys. J.*, 2005, **89**, 4129–4138, DOI: 10.1529/biophysj.105.062695.
9 D. Zhong, S. K. Pal and A. H. Zewail, Femtosecond Studies of Protein-DNA Binding and Dynamics: Histone I, *ChemPhysChem*, 2001, **2**, 219–227.
10 S. Sen, D. Andreatta, S. Y. Ponomarev, D. L. Beveridge and M. A. Berg, Dynamics of water and ions near DNA: comparison of simulation to time-resolved stokes-shift experiments, *J. Am. Chem. Soc.*, 2009, **131**, 1724–1735, DOI: 10.1021/ja805405a.
11 M. A. Berg, R. S. Coleman and C. J. Murphy, Nanoscale structure and dynamics of DNA, *Phys. Chem. Chem. Phys.*, 2008, **10**, 1229–1242, DOI: 10.1039/b715272h.
12 E. B. Brauns, M. L. Madaras, R. S. Coleman, C. J. Murphy and M. A. Berg, Complex local dynamics in DNA on the picosecond and nanosecond time scales, *Phys. Rev. Lett.*, 2002, **88**, 158101.
13 H. Frauenfelder, S. G. Sligar and P. G. Wolynes, The energy landscapes and motions of proteins, *Science*, 1991, **254**, 1598–1603.
14 C. Angell, Formation of Glasses from Liquids and Biopolymers, *Science*, 1995, **267**, 1924–1935.
15 A. Paciaroni, A. Bizzarri and S. Cannistraro, Molecular Dynamics simulation evidences of a boson peak in protein hydration water, *Phys. Rev. E: Stat., Nonlinear, Soft Matter Phys.*, 1998, **57**, R6277–R6280.
16 A. Paciaroni, A. R. Bizzarri and S. Cannistraro, Neutron scattering evidence of a boson peak in protein hydration water, *Phys. Rev. E: Stat., Nonlinear, Soft Matter Phys.*, 1999, **60**, R2476–R2479.
17 T. Li, A. A. Hassanali, Y.-T. Kao, D. Zhong and S. J. Singer, Hydration dynamics and time scales of coupled water-protein fluctuations, *J. Am. Chem. Soc.*, 2007, **129**, 3376–3382, DOI: 10.1021/ja0685957.
18 T. Li, A. Hassanali and S. Singer, Origin of Slow Relaxation Following Photoexcitation of W7 in Myoglobin and the Dynamics of Its Hydration Layer, *J. Phys. Chem. B*, 2008, **112**, 16121, DOI: 10.1021/jp803042u.
19 S. K. Pal and A. H. Zewail, Dynamics of water in biological recognition, *Chem. Rev.*, 2004, **104**, 2099–2123, DOI: 10.1021/cr020689l.
20 S. Pal, J. Peon, B. Bagchi and A. Zewail, Biological water: Femtosecond Dynamics of Macromolecular Hydration, *J. Phys. Chem. B*, 2002, **106**, 12376–12395.
21 S. Bhattacharyya, Z. Wang and A. Zewail, Dynamics of water near a protein surface, *J. Phys. Chem. B*, 2003, **107**, 13218–13228.
22 P. Szendro, G. Vincze and A. Szasz, Pink-noise behaviour of biosystems, *Eur. Biophys. J.*, 2001, **30**, 227–231.
23 A. Bizzarri and S. Cannistraro, Flickering noise in the potential energy fluctuations of proteins as investigated by MD simulation, *Phys. Lett. A*, 1997, **236**, 596–601.
24 A. Bizzarri and S. Cannistraro, Molecular dynamics simulation of plastocyanin potential energy fluctuations: $1/f$ noise, *Phys. A*, 1999, **267**, 257–270.
25 T. G. Dewey and J. G. Bann, Protein dynamics and $1/f$ noise, *Biophys. J.*, 1992, **63**, 594–598.

26 S. K. Pal, L. Zhao, T. Xia and A. H. Zewail, Site- and sequence-selective ultrafast hydration of DNA, *Proc. Natl. Acad. Sci. U. S. A.*, 2003, **100**, 13746–13751, DOI: 10.1073/pnas.2336222100.
27 S. Pal, P. K. Maiti, B. Bagchi and J. T. Hynes, Multiple time scales in solvation dynamics of DNA in aqueous solution: the role of water, counterions, cross-correlations, *J. Phys. Chem. B*, 2006, **110**, 26396–26402, DOI: 10.1021/jp065690t.
28 S. Y. Ponomarev, K. M. Thayer and D. L. Beveridge, Ion motions in molecular dynamics simulations on DNA, *Proc. Natl. Acad. Sci. U. S. A.*, 2004, **101**, 14771–14775, DOI: 10.1073/pnas.0406435101.
29 A. P. Sokolov, H. Grimm, A. Kisliuk and A. Dianoux, Slow Relaxation Process in DNA, *J. Biol. Phys.*, 2001, **27**, 313–327.
30 M. E. Hogan and O. Jardetzky, Internal motions in deoxyribonucleic acid II, *Biochemistry*, 1980, **19**, 3460–3468.
31 T. A. Early and D. R. Kearns, ^{1}H nuclear magnetic resonance investigation of flexibility in DNA, *Proc. Natl. Acad. Sci. U. S. A.*, 1979, **76**, 4165–4169.
32 K. Luger, Dynamic nucleosomes, *Chromosome Res.*, 2006, **14**, 5–16, DOI: 10.1007/s10577-005-1026-1.
33 K. Luger, Structure and dynamic behavior of nucleosomes, *Curr. Opin. Genet. Dev.*, 2003, **13**, 127–135.
34 B. Dorigo, T. Schalch, A. Kulangara, S. Duda, R. R. Schroeder and T. J. Richmond, Nucleosome arrays reveal the two-start organization of the chromatin fiber, *Science*, 2004, **306**, 1571–1573, DOI: 10.1126/science.1103124.
35 D. Roccatano, A. Barthel and M. Zacharias, Structural flexibility of the nucleosome core particle at atomic resolution studied by molecular dynamics simulation, *Biopolymers*, 2007, **85**, 407–421, DOI: 10.1002/bip.20690.
36 S. Sharma, F. Ding and N. V. Dokholyan, Multiscale modeling of nucleosome dynamics, *Biophys. J.*, 2007, **92**, 1457–1470, DOI: 10.1529/biophysj.106.094805.
37 T. C. Bishop, Molecular dynamics simulations of a nucleosome and free DNA, *J. Biomol. Struct. Dyn.*, 2005, **22**, 673–685.
38 K. Voltz, J. Trylska, V. Tozzini, V. Kurkal-Siebert, J. Langowski and J. Smith, Coarse-grained force field for the nucleosome from self-consistent multiscaling, *J. Comput. Chem.*, 2008, **29**, 1429–1439, DOI: 10.1002/jcc.20902.
39 J. Z. Ruscio and A. Onufriev, A computational study of nucleosomal DNA flexibility, *Biophys. J.*, 2006, **91**, 4121–4132, DOI: 10.1529/biophysj.106.082099.
40 T. C. Bishop, Geometry of the nucleosomal DNA superhelix, *Biophys. J.*, 2008, **95**, 1007–1017, DOI: 10.1529/biophysj.107.122853.
41 C. L. White, R. K. Suto and K. Luger, Structure of the yeast nucleosome core particle reveals fundamental changes in internucleosome interactions, *EMBO J.*, 2001, **20**, 5207–5218, DOI: 10.1093/emboj/20.18.5207.
42 J. C. Simó, J. E. Marsden and P. S. Krishnaprasad, The Hamiltonian structure of nonlinear elasticity: The material and convective representations of solids, rods, plates, *Arch. Rat. Mech. Anal.*, 1988, **104**, 125–183.
43 T. C. Bishop, R. Cortez and O. O. Zhmudsky, Investigation of bend and shear waves in a geometrically exact elastic rod model, *J. Comput. Phys.*, 2004, **193**, 642–665.
44 D. Dichmann, Y. Li and J. Maddocks, *Hamiltonian formulations and symmetries in rod mechanics*, in *Mathematical Approaches to Biomolecular Structure and Dynamics (Minneapolis, MN, 1994)*, Springer, New York, 1996, vol. 82 of *IMA Vol. Math. Appl.*, pp. 71–113.
45 D. D. Holm and V. Putkaradze, Nonlocal orientation-dependent dynamics of molecular strands, *C. R. Acad. Sci. Paris*, 2008, submitted.
46 D. Ellis, D. D. Holm, F. Gay-Balmaz, V. Putkaradze and T. Ratiu, Geometric mechanics of flexible strands of charged molecules, *Arch. Rat. Mach. Anal.*, 2008, submitted.
47 R. Kohlrausch, Ueber das Dellmann'sche Elektrometer, *Ann. Phys.*, 1847, **72**, 353.
48 G. Williams and D. Watts, Non-symmetrical Dielectric Relaxation Behavior Arising from a Simple Empirical Decay Function, *Trans. Faraday Soc.*, 1970, **66**, 80–85.
49 B. K. Oksendal, *Stochastic Differential Equations: An Introduction with Applications*, Springer, Berlin–Heidelberg–New York, 5th edn, 2002.
50 Y. L. Klimontovich and J.-P. Boon, Natural Flicker Noise (1/*f* Noise) in Music, *Europhys. Lett.*, 1987, **3**, 395–399.
51 R. Voss and J. Clark, 1/*f* noise in music and speech, *Nature*, 1975, **258**, 317–318.
52 B. Pilgram and D. T. Kaplan, Nonstationarity and 1/*f* noise characteristics in heart rate, *Am. J. Physiol.*, 1999, **276**, R1–R9.
53 A. van der Ziel, Unified Presentation of 1/*f* Noise in Electronic Devices: Fundamental 1/*f* Noise Sources, *Proc. IEEE*, 1988, **76**(3), 233–258.
54 P. G. Collins, M. Fuhrer and A. Zettl, 1/*f* noise in carbon nanotubes, *Appl. Phys. Lett.*, 2000, **76**, 894–896.
55 J. M. Halley, Ecology, evolution and 1/*f*-noise, *Trends Ecol. Evol.*, 1996, **11**, 33–37.
56 Y. Liu, P. Gopikrishnan, P. Cizeau, M. Meyer, C. K. Peng and H. E. Stanley, Statistical properties of the volatility of price fluctuations, *Phys. Rev. E: Stat., Nonlinear, Soft Matter Phys.*, 1999, **60**, 1390–1400.
57 W. Press, Flicker noises in astronomy and elsewhere, *Comments Mod. Phys.*, 1978, **7**, 103–119.
58 R. Voss, Evolution of long-range fractal correlations and 1/*f* noise in DNA base sequences, *Phys. Rev. Lett.*, 1992, **68**, 3805–3808.
59 P. Bak, C. Tang and K. Wiesenfeld, Self-organized criticality: An explanation of the 1/*f* noise, *Phys. Rev. Lett.*, 1987, **59**, 381–384.
60 M. Joyeux, S. Buyukdagli and M. Sanrey, 1/*f* fluctuations of DNA temperature at thermal denaturation, *Phys. Rev. E: Stat., Nonlinear, Soft Matter Phys.*, 2007, **75**, 061914.
61 J. C. Phillips, R. Braun, W. Wang, J. Gumbart, E. Tajkhorshid, E. Villa, C. Chipot, R. D. Skeel, L. Kal and K. Schulten, Scalable molecular dynamics with NAMD, *J. Comput. Chem.*, 2005, **26**, 1781–1802, DOI: 10.1002/jcc.20289.
62 T. E. Cheatham, P. Cieplak and P. A. Kollman, A modified version of the Cornell *et al.* force field with improved sugar pucker phases and helical repeat, *J. Biomol. Struct. Dyn.*, 1999, **16**, 845–862.
63 D. Case, T. Darden, I. T. E. Cheatham, C. Simmerling, J. Wang, R. Duke, R. Luo, K. Merz, B. Wang, D. Pearlman, M. Crowley, S. Brozell, V. Tsui, H. Gohlke, J. Mongan, V. Hornak, P. B. G. Cui, C. Schafmeister, J. Caldwell, W. Ross and P. Kollman, *AMBER 8*, University of California, San Francisco, 2004.
64 A. Perez, I. Marchan, D. Svozil, J. Sponer, T. E. Cheatham, C. A. Laughton and M. Orozco, Refinement of the AMBER force field for nucleic acids: improving the description of alpha/gamma conformers, *Biophys. J.*, 2007, **92**, 3817–3829, DOI: 10.1529/biophysj.106.097782.
65 J. Aqvist, Ion-water interaction potentials derived from free energy perturbation simulations, *J. Phys. Chem.*, 1990, **94**, 8021–8024.
66 T. Fox and P. A. Kollman, Application of the RESP Methodology in the Parametrization of Organic Solvents, *J. Phys. Chem. B*, 1998, **102**, 8070–8079.
67 X.-J. Lu and W. K. Olson, 3DNA: a versatile, integrated software system for the analysis, rebuilding and visualization of three-dimensional nucleic-acid structures, *Nat. Protoc.*, 2008, **3**, 1213–1227, DOI: 10.1038/nprot.2008.104.
68 S. Arnott and D. W. Hukins, Optimised parameters for A-DNA and B-DNA, *Biochem. Biophys. Res. Commun.*, 1972, **47**, 1504–1509.
69 R. E. Dickerson, Definitions and nomenclature of nucleic acid structure parameters, *J. Biomol. Struct. Dyn.*, 1989, **6**, 627–634.
70 W. K. Olson, M. Bansal, S. K. Burley, R. E. Dickerson, M. Gerstein, S. C. Harvey, U. Heinemann, X. J. Lu, S. Neidle, Z. Shakked, H. Sklenar, M. Suzuki, C. S. Tung, E. Westhof, C. Wolberger and H. M. Berman, A standard reference frame for the description of nucleic acid base-pair geometry, *J. Mol. Biol.*, 2001, **313**, 229–237, DOI: 10.1006/jmbi.2001.4987.
71 R. Lavery and H. Sklenar, The definition of generalized helicoidal parameters and of axis curvature for irregular nucleic acids, *J. Biomol. Struct. Dyn.*, 1988, **6**, 63–91.
72 P. K. Mehrotra and D. L. Beveridge, Structural analysis of molecular solutions based on quasi-component distribution functions. Application to [H2CO]aq at 25 °C, *J. Am. Chem. Soc.*, 1980, **102**, 4287–4294.
73 International Technology Laboratory, National Institute of Standards and Technology. See http://www.itl.nist.gov/.

74 *Mathematica, Version 6.0*, Wolfram Research, Inc., Champaign, IL, 2008.
75 *Microcal Origin 7.5*, Microcal Software, Inc., Northampton, MA, 2003.
76 T. C. Bishop, Virtual DNA: A Tool for Investigating the Structure, Flexibility and Dynamics of DNA and Other Fibers, *Bioinformatics*, 2009, in press.
77 K. Luger and T. J. Richmond, DNA binding within the nucleosome core, *Curr. Opin. Struct. Biol.*, 1998, **8**, 33–40.
78 S. K. Pal, L. Zhao and A. H. Zewail, Water at DNA surfaces: ultrafast dynamics in minor groove recognition, *Proc. Natl. Acad. Sci. U. S. A.*, 2003, **100**, 8113–8118, DOI: 10.1073/pnas.1433066100.
79 I. Ohmine, Liquid Water Dynamics: Collective Motions, Fluctuation, Relaxation, *J. Phys. Chem.*, 1995, **99**, 6767–6776.
80 P. Bak, C. Tang and K. Wiesenfeld, Self-organized criticality, *Phys. Rev. A: At., Mol., Opt. Phys.*, 1988, **38**, 364–374.
81 P. Bak, C. Tang and K. Wiesenfeld, Comment on ''Relaxation at the angle of repose'', *Phys. Rev. Lett.*, 1989, **62**, 110.